NOTES AND CORRESPONDENCE

Dispersion of Small-Scale Shear Instabilities

G. CHIMONAS

School of Geophysical Sciences, Georgia Institute of Technology, Atlanta, GA 30332

D. FUA

Instituto di Fisica dell'Atmosfera, 00144 Roma, Italy

27 June 1983 and 14 November 1983

ABSTRACT

Small-scale (Kelvin–Helmholtz) shear instabilities usually display very little dispersion. However, investigations by Hazel reveal an anomalous modal structure when the length scales associated with the density and velocity gradients are sufficiently different. We examine this modal splitting, and discover two distinct families of small-scale waves. The mean phase velocities of the two families can be quite different. The result is of considerable interest in studies of nonlinear interactions among small-scale shear instabilities, since it greatly extends the phase speeds allowed to the resulting disturbances.

1. Introduction

Students are usually introduced to Kelvin–Helmholtz waves through studies of the two-layer model. Two deep homogeneous layers of fluid with a horizontal interface slip past one another. Linearized theory shows that with a sufficiently strong vortex sheet between the layers, perturbations of the interface grow exponentially with time. All these instabilities have the same phase speed along the interface (e.g., Turner, 1973).

This reluctance of Kelvin–Helmholtz waves to disperse persists in more sophisticated calculations. Continuous velocity and density profiles, and rigid lower boundaries produce a far more complex spectrum of shear instabilities. But the smallest scale, fastest growing waves all have phase velocities very close to the wind speed at the height of its inflection point (Einaudi and Lalas, 1974; Lalas and Einaudi, 1976; Davis and Peltier, 1976; Lalas, Einaudi and Fua, 1976). This is not surprising, since Rayleigh's inflection point theorem shows the importance of this wind level, at least to the simplest instabilities. The longer wavelength modes do display some dispersion, but they also have considerably smaller growth rates. This note is entirely concerned with the spectrum of small-scale waves that are the most vigorous of the shear instabilities.

This lack of dispersion among the dominant shear instabilities has immediate consequences for their possible nonlinear interactions. Wavelike boundary layer disturbances, often with quite large amplitudes, are frequently found to have phase-speeds that do not match a wind speed anywhere in the lower troposphere (e.g., Keliher, 1975). Consequently, they cannot be shear instabilities of the flow. But with very few exceptions, there is no mechanism, such as a storm cell, that can be readily identified as having generated them. One obvious suggestion, then would be that these boundary layer modes are excited by nonlinear interaction among the Kelvin–Helmholtz waves. These small-scale instabilities are certainly quite common in the lowest part of the troposphere, and by their very nature must reach amplitudes at which nonlinear effects become important.

If two Kelvin–Helmholtz waves with frequencies and wavenumbers (ω_1, k_1) and (ω_2, k_2) intereact nonlinearly, they produce disturbances with $(\omega_1 + \omega_2, k_1 + k_2)$ and $(\omega_1 - \omega_2, k_1 - k_2)$. But if the basic waves are nondispersive,

$$\frac{\omega_1}{k_1} = \frac{\omega_2}{k_2} = C,$$

the nonlinear disturbances have this same phase speed

$$\frac{\omega_1 + \omega_2}{k_1 + k_2} = \frac{\omega_1 - \omega_2}{k_1 - k_2} = C.$$

Consequently, the nonlinear disturbances and the Kelvin–Helmholtz waves all have a common phase speed and a common critical level. Slight dispersion changes this result only slightly. There is no way that the basic shear instabilities can beat together to excite a boundary layer mode with a phase velocity well outside the limits of the background wind speeds. The above result suggests strong nonlinear interactions across the entire spectrum of the shear instabilities, but it also seems to rule out any resultant generation of the neutral modes of the boundary layer.

The result would be otherwise if several groups of small-scale instabilities with distinct phase speeds could co-exist. It seems possible that such a separation could

happen in a strongly stratified fluid, since then Rayleigh's theorem is significantly modified. We have previously isolated instabilities that exist without any inflection points in the mean velocity profile (Chimonas, 1974; Fua *et al.*, 1976). We therefore decided to seek profiles in which the classical Kelvin–Helmholtz family and these noninflection point waves could closely coexist.

In his fundamental numerical study of shear instabilities, Hazel (1972) discovered that there appeared to be a bifurcation of the modal structure in certain simple model flows. He investigated in some detail the model in which the velocity and stratification profiles were derived from hyperbolic tangent functions. When he allowed the scales for density variations to be considerably smaller than those for the velocity variations, he found twice as many eigensolutions as in the standard model.

If this doubling corresponds to two distinct families of small scale waves, then manipulation of the model parameters might separate their phase speeds. This would produce the result we need to allow the nonlinear scattering into the neutral modes. In Hazel's models, the hyperbolic tangent functions governing wind and density go to zero at the same altitude. For reasons that should become apparent later, we can expect to separate the phase speeds of the two families of small scale instabilities if we displace the two profiles. In the following sections we do just that.

2. Model

Hazel (1972) used the velocity profile

$$U(z) = V \tanh(z/h) \tag{2.1}$$

in conjunction with the Brunt Väisälä frequency N,

$$N^2(z) = \frac{bg}{R}\frac{d}{dz}\tanh(Rz/h). \tag{2.2}$$

This gives a local Richardson number

$$\mathrm{Ri}(z) = \frac{bgh}{V^2}\left[\frac{1}{R}\frac{d\tanh(Rz/h)}{d(z/h)}\right]\left[\frac{d\tanh(z/h)}{d(z/h)}\right]^{-2}. \tag{2.3}$$

When $R > 2$, Ri has a maximum at the origin and approaches zero at large $|z|$. The bifurcation of the modes of instability is found when R is large. Hazel gives detailed results for $R = 5$.

The geometry (2.1), (2.2) has certain disadvantages. All the interesting shears and density gradients concentrate about the origin. The eigenvalues of the two families are almost equal, making the numerical procedures rather unstable. Also, as Hazel notes, too much symmetry in a model may be misleading. Neither the atmosphere nor the ocean will produce such idealized mean states.

We introduce a vertical separation between the density and velocity profiles by combining the flow (2.1) with

$$N^2 = \frac{bg}{R}\frac{d}{dz}\tanh[R(z - z_0)/h]. \tag{2.4}$$

Even with z_0 set at several density scale heights h/R, the anomalous modal structure persists, and it is now more easily studied.

The Richardson number in our flow is

$$\mathrm{Ri}(z) = \frac{bgh}{V^2}\left[\frac{1}{R}\frac{d\tanh[R(z - z_0)/h]}{d(z/h)}\right] \times\left[\frac{d\tanh(z/h)}{d(z/h)}\right]^{-2}. \tag{2.5}$$

Unlike (2.3), this no longer maximizes at $z = 0$. However, it will still be convenient to use the Richardson number at the inflection point as a reference parameter for our calculations:

$$J = \mathrm{Ri}(0). \tag{2.6}$$

The modal problem requires solutions of the equation

$$\frac{d^2w}{dz^2} + \left[\frac{N^2}{(U - C)^2} - \frac{d^2U/dz^2}{(U - C)} - k^2\right]w(z) = 0, \tag{2.7}$$

subject to appropriate boundary conditions [Hazel 1972, Eq. (1.1).] Instabilities correspond to eigenvalues C with a positive imaginary part. (The real part of C is the horizontal phase speed of the mode.)

The profiles (2.1), (2.4) rapidly approach limiting values at large $|z|$. This allows us to smoothly join them to outer regions in which N^2 and U have constant values. Boundary conditions are then easily applied in these outer regions. We test our selection of the heights at which the inner and outer domains join, by increasing the inner domain until the eigenvalue problem becomes insensitive to further increases.

Calculations are performed in the nondimensionalized space of $y = z/h$, $c = C/V$ and $\alpha = kh$. The eigenvalue problem is then completely specified by assigning values to J and z_0/h.

3. Results

We find that there are enough similarities between Hazel's results and ours to allow sensible comparisons. There are also obvious differences. The symmetry in Hazel's model produces either stationary modes or oppositely traveling wave pairs. Our model does not share this behavior.

We present the results of our calculations for the parameter choice $R = 12$ and $z_0/h = \frac{1}{3}$ or $\frac{1}{6}$. In this scheme the velocity and density length scales are very different and the maximum of the Brunt Väisälä fre-

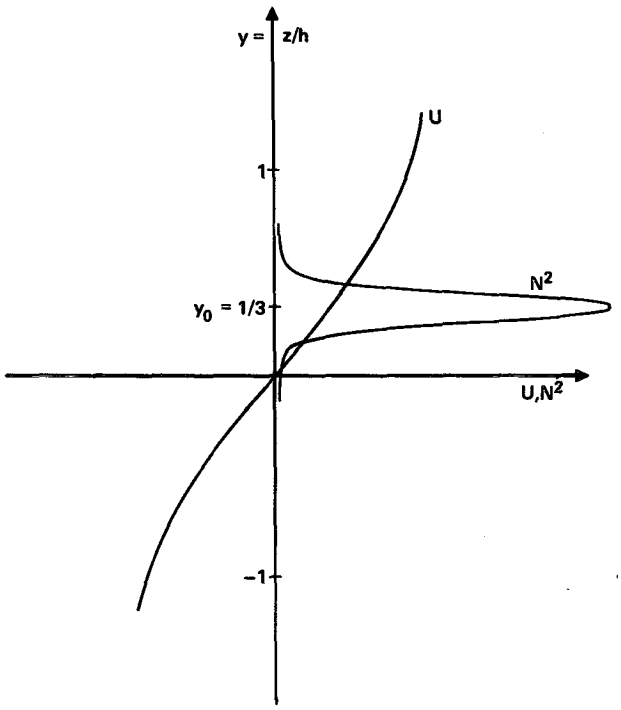

FIG. 1. The model profiles of wind U and Brunt-Väisälä frequency N, used in the calculations. Shown are $U = V \tanh(y)$ and $N^2 = A^2 \times \text{sech}^2 R(y - y_0)$ with $R = 12$ and $y_0 = \frac{1}{3}$.

quency is well separated from the velocity inflection point. These profiles are illustrated in Fig. 1. All results are given in terms of the nondimensional functions $y = z/h$, $c = C/V$ and $\alpha = kh$.

Figures 2 and 3 are plots of c_i the imaginary part of eigenvalue c, against wavenumber α, for two distinct modes that can co-exist in the flow. The growth rate σ for the mode is easily derived from the display, since $\sigma = \alpha c_i$. These figures show that the growth rate varies rapidly with the Richardson number. As J falls from 0.4 to 0.1 in these plots, c_i increases by a factor greater than 10. For the more symmetric models with $y_0 = 0$, the growth rate on a locus of fixed J maximizes around $\alpha = 0.5$ (Hazel, 1972, Fig. 1). In the present system, this is also the case for the more unstable regions, but there is considerable departure from this trend for larger J. However, it is clear that the fastest growing waves are scaling with the velocity profile, not with the density profile which is shorter by a factor of 12. Fig. 3 shows that halving the separation y_0 changes the results quantitatively but leaves their main features qualitatively unaltered.

The curves of neutral stability in α, J space could not be accurately determined. We did not specifically compute singular neutral modes, but attempted to obtain contours of the eigenmodes c_i. The locus of the limit $c_i \to 0$ would give the stability boundaries, but we could not approach these boundaries with acceptable accuracy. Fig. 4 shows parts of these contours and demonstrates the difficulty. The convergence is very slow. The contour of $c_i = 10^{-3}$ locates growth rates that are nearly two orders of magnitude smaller than the maximum of c_i in the plane. Even so, the contour for $c_i = 10^{-4}$ is still very different from the 10^{-3} contour, and at such small values the computations become increasingly difficult and expensive. These results indicate that neutral stability curves must be viewed with some caution, since a large fraction of the "unstable" area can correspond to insignificant growth rates.

Our interest is in the areas where two distinct modes co-exist. It can be seen from Fig. 4 that two modes, designated Mode 1 and Mode 2, occupy a common region of the J/α diagram. The co-existence includes the regions of largest growth rates for both modes. The structure of these co-existing modes is displayed in Fig. 5 for a wavenumber α close to that corresponding to maximum growth for the specified shear flow. So, to the extent that the growth rates of linear theory are significant, these are the eigenmodes that would be expected to dominate the wave activity.

The main difference between Modes 1 and 2 is the location of their critical levels. Mode 1, which is the

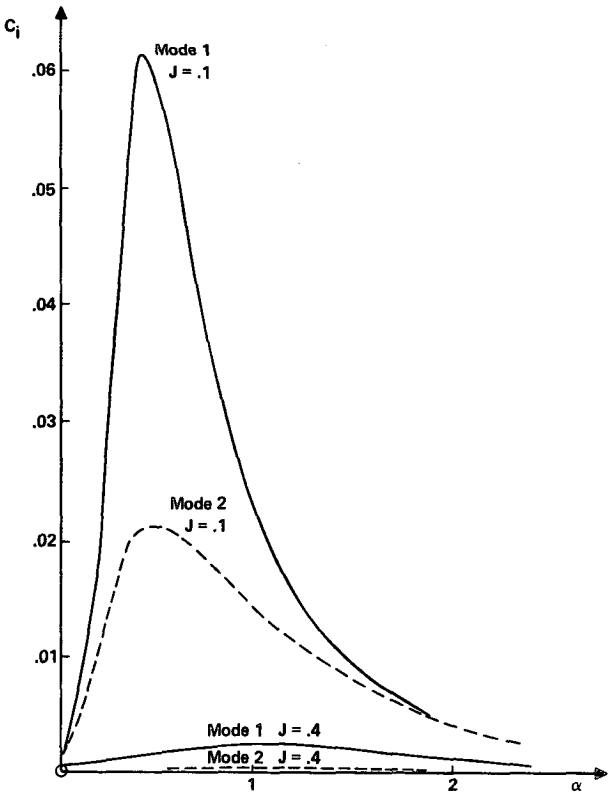

FIG. 2. Plots of the imaginary parts of horizontal phase speed c_i against wavenumber α for modes of the flow displayed in Fig. 1. Growth rates σ are computed from $\sigma = \alpha c_i$. Two buoyancy states $J = 0.1$ and $J = 0.4$ have been used [See Eq. (2.6)].

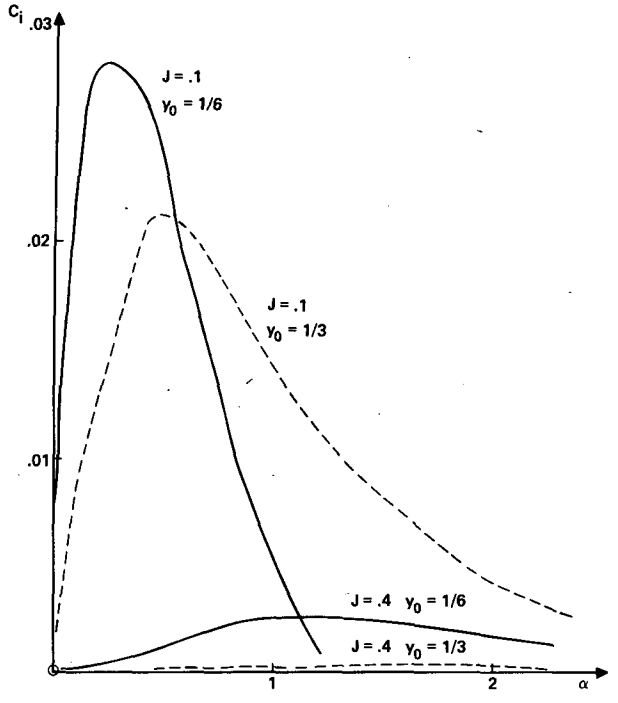

FIG. 3. Effects of changing the separation of y_0 [Eq. (2.4)], ($y_0 = z_0/h$). Curves for Mode 2 are shown for two choices of y_0.

faster growing of the pair, has a critical level close to the inflection point $U'' = 0$ of the wind profile. Mode 2, on the other hand, has its critical level high in the tail of the Brunt Väisälä frequency profile on the side remote from the inflection. Nothing in the amplitude or phase profiles of Mode 2 indicates that the change of wind curvature affects this eigenmode.

On this basis we tentatively identify Mode 1 as the conventional Kelvin–Helmholtz instability. Its growth rate is considerably greater than the growth rate of Mode 2, so it is the dominant instability of linearized theory. Mode 2 seems to be of a rather different nature. It may correspond more closely with modes that can exist in inflection free profiles with sufficiently strong bouyancy gradients (Chimonas 1974, Fua *et al.*, 1976). Rayleigh's theorem only demands an inflection point for instability if the flow is unstratified (Drazin and Howard, 1966).

Although the wind shear is responsible for generating the waves and determining their length scales, the region of large bouyancy is responsible for much of their structure. In particular, the phase changes and internal minima of the modes occur over the interval where N^2 is large.

Along the two axes $J = 0$ and $\alpha = 0$, our results depart from those of Hazel. We do not find a stability boundary on $J = R\alpha$. This is not too surprising since we have lost the symmetries that give special significance to the zero of phase speeds. However, there must be a stability boundary starting at $J = 0$, $\alpha = 1$ and lying near to the abscissa. Our numerical routines were not suitable for use in the regions of very small J and c_i. We obtained eigenmodes for $1 < \alpha < 4$ as close to

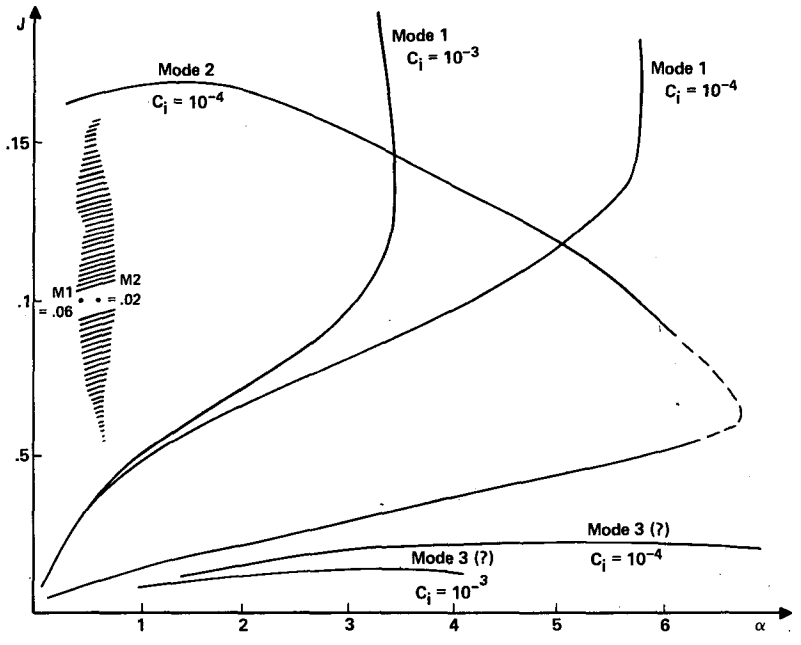

FIG. 4. Stability contours in the J, α plane. The Mode 1 contours return very close to the ordinate. Mode 3 contours are believed to close back on lines very near $J = 0$. The shaded area indicates the ridge in the c_i contours. Spot values for c_i are shown for Modes 1 and 2 (M1, M2). The display is for $y_0 = \frac{1}{3}$.

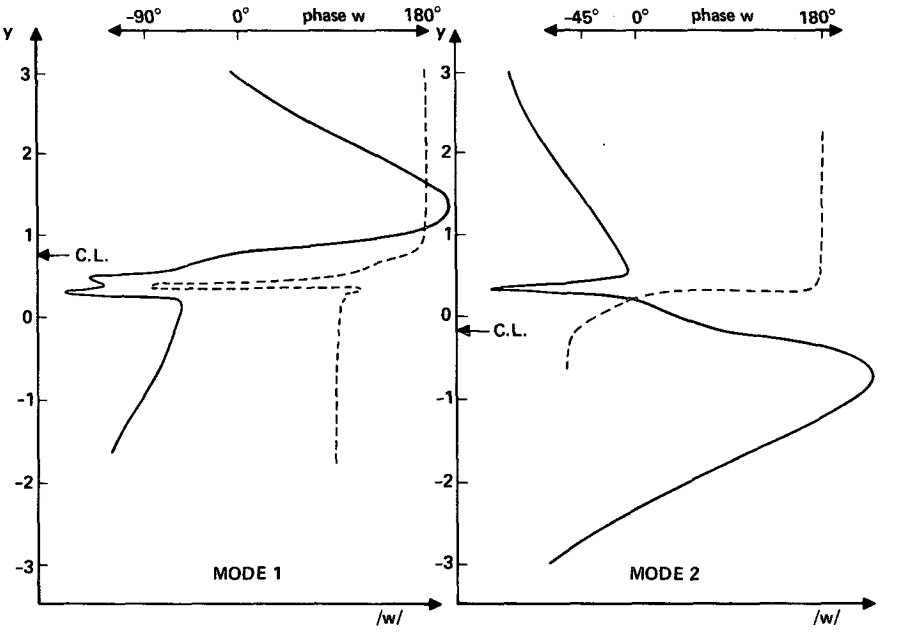

FIG. 5. Structures of Mode 1 and Mode 2 for $J = 0.1$, $y_0 = \frac{1}{3}$, $\alpha = 0.6$. The height of the critical level of each mode is indicated. The profiles display properties of w, the vertical component of the fluid velocity. The solid lines correspond to the modulus of w; the dashed lines to its phase.

the $J = 0$ axis as we could go with our programs. It is not clear whether these eigenmodes at very small J are a continuation of Mode 1, or an independent third mode.

When the amplitudes of the modes are large enough to demand attention to nonlinear effects, some interesting features emerge. Specifically, the interaction between the two types of mode excites disturbances that can have horizontal phase speeds quite different from the speeds of the modes themselves. This is illustrated in Figs. 6 and 7. In Fig. 6 we plot the phase speeds of modes 1 and 2 as functions of horizontal wavenumber. Apart from some minor structure, each mode shows very little phase speed change with wave length. However, there is a clear separation between the speeds of the modes at all wavenumbers.

Consider the result of the interaction between Mode 1 (phase speed C_1 and wavenumber α_1) and Mode 2 (phase speed C_2 and wavenumber α_2). The horizontal phase speed of the nonlinear response is

$$C_r' = [C_1\alpha_1 - C_2\alpha_2]/(\alpha_1 - \alpha_2). \qquad (3.1)$$

This speed C_r' is a very strong function of (α_1, α_2). Its full plot requires the three-dimensional space $(C_r', \alpha_1, \alpha_2)$, but we can illustrate with a projection on some plane. We have chosen to fix the Mode 1 at the location marked Z in Fig. 6 (i.e., $\alpha_1 = 1.5$), and then scan over the range of Mode 2. The result is shown in Fig. 7. The nonlinear excitation assumes a phase speed that passes through almost all possible values $(-\infty, +\infty)$ as α_2 passes through its range.

Consequently, it is quite possible for the primary instabilities, Modes 1 and 2, to co-operatively excite boundary layer disturbances with phase speeds outside the range of the mean wind field. These could be neutral modes of the boundary layer, which of course do not have critical levels and cannot be generated directly by the wind shear. However, there is the possibility now that they result in this indirect manner from the wind shear instability.

A note of caution is in order. As one referee (WLJ) has noted, there is more to nonlinear interaction than just a matching of the phase speeds. In particular, the various eigensolutions must have some spatial overlap. Since both Modes 1 and 2 are very restricted in altitude, the vertical separation that produces their different phase speeds must not be so great as to prevent also their spatial overlap. We can always produce model profiles with the properties that support our theoretical requirements. Nevertheless, whether or not such profiles exist in nature is quite another matter.

4. Discussion and conclusions

The bifurcation of modes discovered by Hazel results from a family of instabilities associated with large bouyancy gradients. Unlike the Kelvin–Helmholtz waves, the new modes are not confined to the inflection

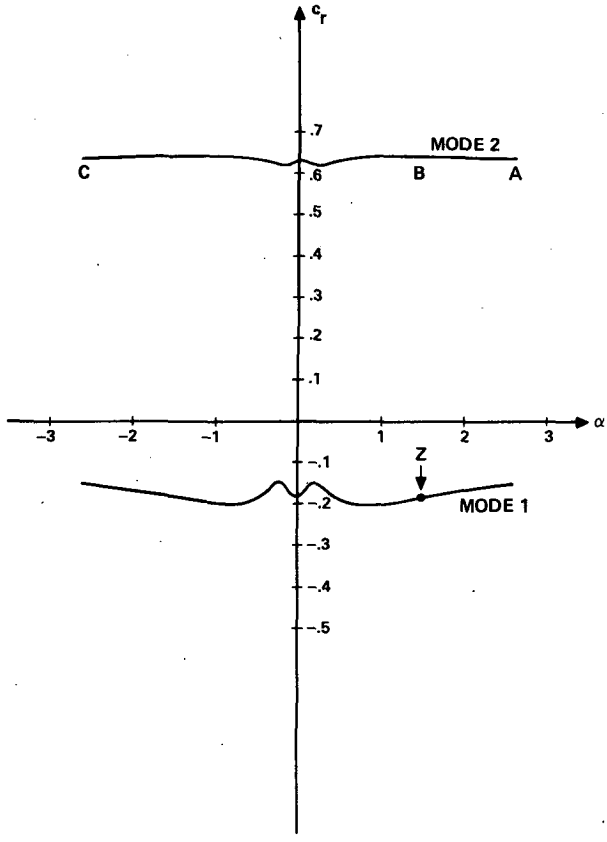

FIG. 6. The horizontal phase speeds C_r of the modes as a function of wavenumber α. Plots are given for $J = 0.1$ and $y_0 = \frac{1}{3}$.

point of the velocity profiles. Rather, they are located where the bouyancy gradients are largest. Consequently, as we separate the maxima of velocity gradients and buoyancy gradients, the two families assume distinct phase speeds.

The instabilities at the velocity inflection point grow faster than the second family of instabilities, but only by a factor of 3 or less. So, both families can reach large amplitudes within the same general time span. The difference of phase speeds of the two families allows nonlinear excitation of disturbances with almost any phase speed. For now $(\omega_1 - \omega_2)/(k_1 - k_2)$ will approach zero as the frequencies approach the same value, and $\pm\infty$ as the wavenumbers approach a common value. Of course many other factors must be considered before a desired nonlinear excitation can be achieved, but this factor was our immediate concern. It is also worth noting that the nonlinear excitation resulting from the differencing of wavenumbers, $k_1 - k_2$, leads to a disturbance with a much larger wavelength than the primary instabilities. This, again, is required in the present context, since the neutral modes of the boundary layer typically have much larger dimensions than the Kelvin–Helmholtz waves. Calculations of the nonlinear excitation strength will be presented at a later date.

Finally, it is necessary to question the physical model adopted in this paper. We do not mean the use of idealizations such as tangent hyperbolic functions; this is a standard technique. It reflects the belief that flow stability depends on general features such as Richardson's numbers, inflection points and profile tendencies rather than very specific and limited geometries. But it is only reasonable to ask whether the atmosphere should allow density gradient scales that are an order of magnitude smaller than velocity gradient scales, and further, whether the two profiles can be separated, as required in these calculations. Really, theoretical arguments on these points cannot be conclusive. Only sufficiently accurate and extensive field observations could settle such a debate. As yet, such observations are almost impossible. Step-like changes in velocity and temperature are observed in the boundary layer, both internally and at capping inversions, but their detailed structure has not been resolved.

However, we would suggest that at least one mechanism exists to produce sharp temperature changes that do not coincide with local velocity inflections. It depends on the presence of water substance. Balloon

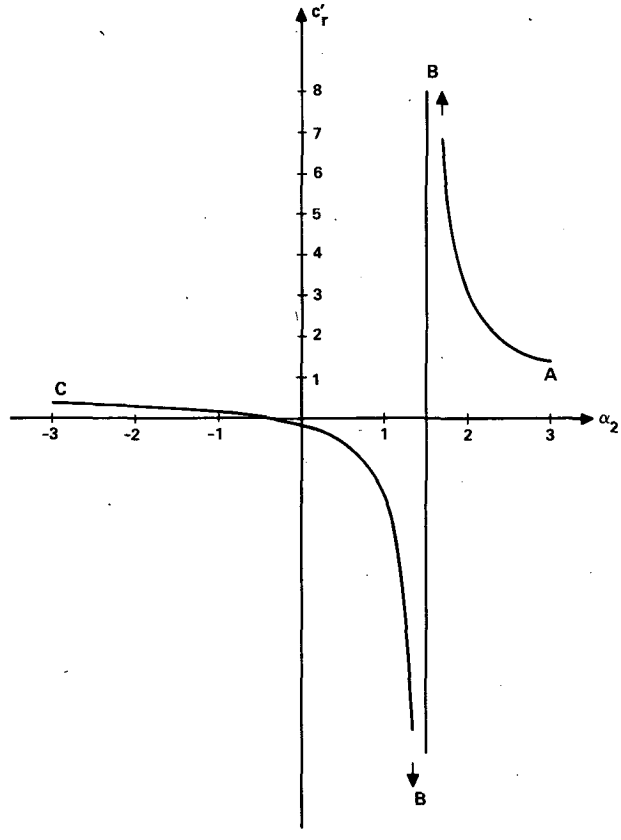

FIG. 7. The horizontal phase speed C'_r of the disturbance excited by nonlinear interaction between Mode 1 with wavenumber $\alpha_1 = 1.5$ and Mode 2 with the shown range of wavenumber α_2. Plots are given for $J = 0.1$ and $y_0 = \frac{1}{3}$.

soundings of the boundary layer frequently reveal sharp changes of water content. Changes correspond to interfaces between distinct air masses, one flowing over the other. Assuming a similarity in the diffusion of water vapor and momentum, we note that the scale length for the interface will also be found in the wind profile.

A second scale length will be found if the damper layer passes from unsaturated to saturated water vapor pressure at some height. Saturation vapor pressure is a very sensitive function of temperature, and the coupling between radiation and the atmospheric gas can depend heavily on water droplets or the water complexes on aerosols. Consequently, the region of phase transitions can have associated strong temperature gradients. The mechanisms determining the scale and location of this temperature (i.e., bouyancy) interface are certainly not identical with those producing the velocity interface. It is conceivable, although by no means certain, that this could lead to the type of profile studied in this note.

Acknowledgment. This work was supported in part by the Atmospheric Sciences Section of the National Science Foundation through Grant ATM-8317367.

REFERENCES

Chimonas, G., 1974: Considerations of the stability of certain heterogeneous shear flows including some inflexion-free profiles. *J. Fluid Mech.*, **65,** 65–69.

Davis, P. A., and W. R. Peltier, 1976: Resonant parallel shear instability in the stably stratified planetary boundary layer. *J. Atmos. Sci.*, **33,** 1287–1300.

Drazin, P. G., and L. N. Howard, 1966: Hydrodynamic stability of parallel flow of inviscid fluid. *Advances in Applied Mathematics,* Vol. 9, Academic Press, 1–89.

Einaudi, F., and D. P. Lalas, 1974: Some new properties of Kelvin–Helmholtz waves in an atmosphere with and without condensation effects. *J. Atmos. Sci.*, **31,** 1995–2007.

Fua, D., F. Einaudi and D. P. Lalas, 1976: The stability analysis of an inflexion-free velocity profile and its application to the nighttime boundary layer. *Bound.-Layer Meteor.*, **10,** 35–54.

Hazel, P., 1972: Numerical studies of the stability of inviscid stratified shear flows. *J. Fluid Mech.*, **51,** 39–61.

Keliher, T. E., 1975: The occurrence of microbarograph-detected gravity waves compared with the existence of dynamically unstable wind shear layers. *J. Geophys. Res.*, **80,** 2967–2796.

Lalas, D. P., and F. Einaudi, 1976: On the characteristics of gravity waves generated by atmospheric shear layers. *J. Atmos. Sci.*, **33,** 1248–1259.

——, —— and D. Fua, 1976: The destabilizing effect of the ground on Kelvin–Helmholtz waves in the atmosphere. *J. Atmos. Sci.*, **33,** 59–69.

Turner, J. S., 1973: *Buoyancy Effects in Fluids,* Chap. 4, Cambridge University Press, p. 94.